

Revisiting *Hypostomus khimaera* (Siluriformes: Loricariidae): the identity of a morphologically variable species



Correspondence:
Vandergleison de Carvalho
dcarvalhojet@hotmail.com

Vandergleison de Carvalho¹, Victória Joana da Silva Müller²,
 Daniela Cristina Ferreira^{2,4}, Cláudio Henrique Zawadzki³ and
 Luiz Fernando Caserta Tencatt⁴

Hypostomus khimaera, described from the upper rio Paraguai basin in Brazil, was reported to present some morphological variations in its original description, which allied to its relatively wide geographical distribution reinforced the need for a new assessment of its taxonomic status. Here, we analyzed a new robust set of material, composed by 636 specimens from several localities within the upper rio Paraguai basin, besides the material listed in the original description. From this, it was possible to better understand the limits of the species providing a more accurate diagnosis and a redescription for *H. khimaera*, which also brought some light to the limits of the *H. cochliodon* group itself. The species can be distinguished from its congeners by having the following features: (I) absence of a notch between the metapterygoid and hyomandibula, (II) acutely angled dentaries, with up to about 90°, (III) teeth with medial cusp ranging from villiform to shovel-shaped, (IV) opercle completely surrounded by a thick layer of skin, (V) a longitudinal dark stripe along middle portion of flanks, which is variably diffuse, and (VI) dark spots on at least one part of the body. Although morphological and color pattern differences have been found in different populations along the upper rio Paraguai basin, all examined specimens are herein considered to belong to *H. khimaera*, a decision based on both morphologic and molecular analyses. Additionally, an updated identification key for the *Hypostomus* species in the Brazilian portion of the upper rio Paraguai basin is also provided.

Keywords: Armored catfish, *Hypostomus cochliodon*, Identification key, Rio Paraguai basin, Taxonomy.

Submitted June 25, 2024

Accepted July 15, 2024

by Carlos DoNascimento

Epub September 23, 2024

Online version ISSN 1982-0224

Print version ISSN 1679-6225

Neotrop. Ichthyol.

vol. 22, no. 3, Maringá 2024

¹ Departamento de Vertebrados, Setor de Ictiologia, Museu Nacional, Universidade Federal do Rio de Janeiro, Quinta da Boa Vista s/n, São Cristóvão, 20940-040 Rio de Janeiro, RJ, Brazil. (VC) dcarvalhojet@hotmail.com (corresponding author).

² Laboratório de Genética e Citogenética Animal, Universidade Federal de Mato Grosso, Instituto de Biociências, Av. Fernando Corrêa da Costa, 2367, Boa Esperança, 78060-900 Cuiabá, MT, Brazil. (VJSM) mullersjv@gmail.com, (DCF) ferreiradc@gmail.com.

³ Departamento de Biologia, Núcleo de Pesquisas em Limnologia, Ictiologia e Aquicultura, Universidade Estadual de Maringá, Av. Colombo, 5790, 87020-900 Maringá, PR, Brazil. (CHZ) chzawadzki@hotmail.com.

⁴ Departamento de Biologia e Zoologia, Instituto de Biociências, Universidade Federal de Mato Grosso, Av. Fernando Corrêa da Costa, 2367, Boa Esperança, 78060-900 Cuiabá, MT, Brazil. (LFCT) luitencatt@hotmail.com.

Hypostomus khimaera, descrita da bacia do alto rio Paraguai no Brasil, apresentou algumas variações morfológicas em sua descrição original, o que, aliado à sua distribuição geográfica relativamente ampla, reforçou a necessidade de uma nova avaliação de seu status taxonômico. Aqui, nós analisamos um novo conjunto robusto de material, composto por 636 exemplares de diversas localidades da bacia do alto rio Paraguai, além do material listado na descrição original. A partir disso, foi possível compreender melhor os limites da espécie, proporcionando um diagnóstico mais preciso e uma redescricao de *H. khimaera*, que também trouxe alguma luz aos limites do próprio grupo *H. cochliodon*. A espécie pode ser distinguida de suas congêneres por apresentar as seguintes características: (I) ausência de um entalhe entre o metapterigóide e a hiomandíbula, (II) dentários agudamente angulados, com cerca de até 90°, (III) dentes com cúspide medial variando de viliforme a em forma de pá, (IV) opérculo completamente margeado por uma espessa camada de pele, (V) uma faixa escura longitudinal ao longo da porção média dos flancos, que é variavelmente difusa, e (VI) manchas escuras em pelo menos uma parte do corpo. Embora diferenças morfológicas e de padrão de cor tenham sido encontradas em diferentes populações ao longo da bacia do alto rio Paraguai, todos os espécimes examinados são aqui considerados como pertencentes à *H. khimaera*, uma decisão baseada em ambas análises morfológicas e moleculares. Adicionalmente, uma chave de identificação atualizada para as espécies de *Hypostomus* da porção brasileira da bacia do alto rio Paraguai também é fornecida.

Palavras-chave: Bacia do rio Paraguai, Cascudo, Chave de identificação, *Hypostomus cochliodon*, Taxonomia.

INTRODUCTION

Loricariidae is composed by suckermouth armored catfishes widely distributed within the Neotropical region, being natively recorded from Central America to South America (Reis *et al.*, 2003; Armbruster, 2004). Currently, this family represents the fifth largest vertebrate group on planet Earth, with around 115 valid genera and more than 1.050 valid species (Zawadzki *et al.*, 2018; Fricke *et al.*, 2024). Hypostominae is its most diverse subfamily, harboring around 510 species grouped into 45 genera (Fricke *et al.*, 2024), with *Hypostomus* Lacépède, 1803 as its largest genus, containing more than 150 valid species (Zawadzki *et al.*, 2016, 2018, 2020a,b, 2021; Oliveira *et al.*, 2020; Penido *et al.*, 2023).

Among the Loricariidae, two groups are considered unique among fish and other vertebrates due to their xylophagous feeding habits, *Panaque* Eigenmann & Eigenmann (1889) and the species of the *Hypostomus cochliodon* Kner, 1854 group *sensu* Armbruster (2003) (Schaefer, Stewart 1993; Armbruster 2003; McDonald *et al.*, 2015). Both have representatives with teeth morphologically adapted for wood consumption, with an appearance similar to that of a spoon/ladle. However, not all species of the *Hypostomus cochliodon* group have teeth with such specialization. *Hypostomus hemicochliodon* Armbruster, 2003 and *H. khimaera* Tencatt, Zawadzki & Froehlich, 2014, possess shovel-shaped/spatulate teeth, *i.e.*, teeth with broad medial cusp, but not conspicuously

concave, an intermediary condition between the villiform teeth of most congeners and the typical spoon-shaped teeth of the species within the *H. cochliodon* group (see Armbruster, 2003, 2004; Tencatt *et al.*, 2014).

Species of the *H. cochliodon* group can be diagnosed from other congeners by the following synapomorphies: (I) absence of a notch between the metapterygoid and the hyomandible (*vs.* presence), (II) dentary tooth rows sharply angled, with less or approximately 90° (*vs.* dentary teeth rows obtusely angled, generally greater than 90°), and (III) teeth with a spoon- or spatula-shaped medial cusp (= intermediate tooth in Armbruster (2003) (*vs.* villiform teeth) (Armbruster, 2004; Armbruster, Souza, 2005; Tencatt *et al.*, 2014; Zawadzki, Hollanda Carvalho, 2014). Additionally, Tencatt *et al.* (2014) discussed the degree of development and/or exposure of the opercle as a possible way of recognizing species from the *H. cochliodon* group (less developed and/or internalized in the *H. cochliodon* group *vs.* more developed and/or externalized in remaining congeners).

Following the revisionary study by Armbruster (2003), a series of works raised the number of valid species of the *H. cochliodon* group from 11 to 22, doubling the representatives for the group in the last 21 years (Armbruster, Souza, 2005; Hollanda Carvalho, Weber, 2004; Hollanda Carvalho *et al.*, 2010; Tencatt *et al.*, 2014; Oliveira *et al.*, 2020). Furthermore, the geographic distribution of the group was considerably expanded, with records in the river systems of the Amazon, La Plata and coastal rivers of Venezuela, such as the Cuyuni, Orinoco Aroa, Tucuyo, Yaracuy and Lago de Maracaibo, of the Guyana in the rivers Essequibo, Takutu and Ireng, and of Colombia in the rivers Atrato, Sinú and Magdalena (Armbruster, 2003; Hollanda Carvalho, Weber, 2004; Armbruster, Souza, 2005; Hollanda Carvalho *et al.*, 2010; Tencatt *et al.*, 2014; Zawadzki, Hollanda Carvalho, 2014; Oliveira *et al.*, 2020; Fricke *et al.*, 2024).

The rio Amazonas basin has the highest species richness of the *H. cochliodon* group, with 13 valid species (Hollanda Carvalho *et al.*, 2010; Tencatt *et al.*, 2014; Zawadzki, Hollanda Carvalho, 2014). Contrasting with this, only three species of this group are known to occur in the rio de La Plata basin: *H. basilisko* Tencatt, Zawadzki & Froehlich, 2014, apparently endemic to tributaries of the rio Miranda in the Bodoquena Plateau, Mato Grosso do Sul, Brazil; *H. cochliodon*, widely distributed in the Paraná-Paraguai system; and *H. khimaera*, with relatively wide distribution within the upper rio Paraguai basin in the states of Mato Grosso and Mato Grosso do Sul, and potentially present in this same basin in Bolivian and Paraguayan territories. Additionally, *H. khimaera* was recently recorded in a tributary of the upper rio Paraná basin in Mato Grosso do Sul State, extending the geographic distribution of this species to the Paraná-Paraguai River system, although considerably less widespread than *H. cochliodon* (Lopes *et al.*, 2024).

Tencatt *et al.* (2014), in the taxonomic review of *H. cochliodon*, reported morphological variation in specimens of *H. khimaera*, such as tooth morphology and degree of development of odontodes and keels on trunk bony plates. According to those authors, these morphological variations were observed not only when comparing different populations but also among specimens of the same population (see Tencatt *et al.*, 2014:600). Within the decade after its original description, many recently collected or previously non examined material of *H. khimaera* has been discovered, allowing us to revisit the taxonomy of *H. khimaera* and to provide new insights on its taxonomy. After the analysis of the specimens listed by Tencatt *et al.* (2014) plus additional material

from other localities within the upper rio Paraguai basin, it was possible to better delimit *H. khimaera* and attest that the observed morphological differences are not sufficient to diagnose any new species, which was also corroborated by molecular data. As a result, its original diagnosis and description have become inaccurate. Therefore, the aim of this study is to provide a new diagnosis and redescription for *H. khimaera*. Additionally, we also provided an updated identification key for the species of *Hypostomus* from the upper rio Paraguai basin based on Tencatt (2022).

MATERIAL AND METHODS

Morphological analysis. Measurements were taken point-to-point with a digital caliper with an accuracy of 0.1 mm. Measurements and counts follow Boeseman (1968), with modifications from Weber (1985) and Zawadzki *et al.* (2008, 2018). Standard length (SL) and total length (TL) are expressed in millimeters, and the rest of the measurements are expressed as percent relative to the standard length or head length (HL) in the case of subunits of head. All measurements were obtained from the left side of the specimens, whenever possible. Nomenclature and counts of bony plates follow Schaefer (1997), with modifications from Oyakawa *et al.* (2005). Osteological analysis was performed using cleared and stained (c&s) specimens according to the protocol of Taylor, Van Dyke (1985). The terminology of laterosensory canals and bones follows Schaefer (1987; 1997). In the description, counts indicated with an asterisk refer to the holotype. Counts in the description include the type material (holotype and 19 paratypes), provided by Tencatt *et al.* (2014), with the addition of 33 non-type specimens analyzed herein. Regarding color pattern, in specimens with diffuse longitudinal dark stripe, the visualization was better achieved by submerging the specimens in water or alcohol, enhancing the contrast between colors. Abbreviations of institutions follow Sabaj (2020), except for CITL, Coleção Ictiológica de Três Lagoas, Três Lagoas, Mato Grosso do Sul, Brazil.

Molecular analysis. The total DNA was extracted from seven specimens of *H. khimaera* from the upper rio Paraguai basin, from which the sequences were deposited on GenBank database. One of these specimens was collected in a tributary of the rio Coxipó-açu (CPUFMT 8345; PP998996), two from a tributary of the rio Cuiabá (CPUFMT 8344; PP998994 and PP998995), both localities in Mato Grosso State, plus one in the córrego Último Gole (CPUFMT 8346; PP998997), one in the córrego Criminoso (CPUFMT 8347; PP998998), and two in the córrego Fortaleza (CPUFMT 8348; PP998999 and PP999000), the last three localities in Mato Grosso do Sul State. Additionally, sequences obtained from other *Hypostomus* species for comparison purposes were extracted from BOLD to compose the dataset analyzed for species delimitation, namely: *H. ancistroides* (Ihering, 1911) (FUPR616–09 and FUPR617–09), *H. affinis* (Steindachner, 1877) (MUCU027–13 and MUCU035–13), *H. alatus* Castelnau, 1855 (BSB292–10 and BSB297–10), *H. albopunctatus* (Regan, 1908) (FUPR552–09 and FUPR554–09), *H. auroguttatus* Kner, 1854 (FPSR122–09 and FPSR129–09), *H. brevis* (Nichols, 1919) (FUPR557–09 and FUPR559–09), *H. commersoni* Valenciennes, 1836 (LARI218–13 and LARI229–13), *H. heraldoi* Zawadzki, Weber & Pavanelli, 2008

(FUPR591–09 and FUPR596–09), *H. gymnorhynchus* (Norman, 1926) (GBO1154–16 and GBO2461–17), *H. paulinus* (Ihering, 1905) (FUPR577–09 and FUPR578–09). The extraction technique followed the protocol described by Aljanabi, Martinez (1997). The COI gene was amplified using the primers COI FISH F1 and FISH R1 described by Ward *et al.* (2009). The reagents and cycling conditions were the same as those described by Arruda *et al.* (2019). The amplicons of the COI gene were purified and sequenced by Biotecnologia Pesquisa e Inovação (BPI, <https://bpibiotecnologia.com.br>). The samples were purified using a magnetic bead kit of the AMPure XP type, and sequenced with a BigDye® Terminator v. 3.1 Cycle Sequencing kit (Applied Biosystems), following the manufacturer's protocols. The samples were sequenced automatically by capillary electrophoresis in an ABI3730xl Genetic Analyzer (Applied Biosystems).

Data analysis. The raw sequences were edited and the presence of gaps was verified in Geneious® 7.1.3 (Kearse *et al.*, 2012), while the sequences were aligned in Mega v. 11 (Tamura *et al.*, 2021) using the ClustalW algorithm (Thompson *et al.*, 2003). The aligned sequences were inspected in MEGA for the identification of stop codons, pseudogenes, and deletions and insertions. The mean intraspecific and interspecific genetic distances between the morphospecies and the consensus MOTUs were calculated in Mega v. 11 using the Kimura-2-Parameter (K2P) model (Kimura, 1980), following Hebert *et al.* (2004), who employed the minimum interspecific and the maximum intraspecific distances identified in Excel, using the Minimum and Maximum functions. The Molecular Operational Taxonomic Units (MOTUs) were identified in the JMotu software (Jones *et al.*, 2011) based on the Optimum Threshold (OT). The OT was calculated in the SPIDER (SPecies IDentify and Evolutions in R, Brown *et al.* (2012) package using the “LocalMinima” function in the R environment v. 3.6.3 (<https://www.r-project.org>; R Development Core Team, 2016). The groups formed by the Assemble Species by Automatic Partitioning software (ASAP, Puillandre *et al.*, 2021) were estimated at the site <https://bioinfo.mnhn.fr/abi/public/asap/asapweb.html> using the K2P substitution model, with all other parameters at the default values. The Bayesian ultrametric input tree used for the Generalized Mixed Yule Coalescence (GMYC) method was constructed in BEAST2 (version available at CIPRES) with the following parameters: HKY+G model, gamma shape, relaxed molecular clock with lognormal distribution, and the birth-death speciation model, which was run three times independently, initiated using random trees, each with 50 million generations, based on the Markov Chain Monte Carlo (MCMC), with 25% of the topologies being discarded as burn-in during each run. The results of the three runs were combined in LogCombiner v. 2. Effective Sample Size (ESS > 200) was verified in Tracer v. 1.6. The three files with the tree extension were combined in Treeannotator v. 1.8 (version available at CIPRES), visualized in FigTree v. 1.4, and exported with a NEWICK final extension. This final tree was used in the GMYC analysis, which was run in the SPLITs (SPecies LIimits by Threshold Statistics; Monaghan *et al.*, 2009) package in the R environment v. 3.6.3, using a single threshold model.

RESULTS

Hypostomus khimaera Tencatt, Zawadzki & Froehlich, 2014

(Figs. 1–8, 11; Tab. 1)

Hypostomus cochliodon (non Kner, 1854). —Armbruster, 2003:19, 21–25 (*partim*; identification key; redescription).

Hypostomus khimaera. —Tencatt *et al.*, 2014:597–600 (original description; type-locality: córrego Salobo (= Salobro)). —Oliveira *et al.*, 2020:493, 496 (diagnosed from *H. labyrinthus*; listed as comparative material). —Carvalho *et al.*, 2019:50, 52 (brief description; photo in life). —Lopes *et al.*, 2024:594–99 (new record; diagnosis; photos in life; geographic distribution).



FIGURE 1 | Holotype of *Hypostomus khimaera*, MZUSP 111129, 139.1 mm SL, córrego Salobo, rio Paraguai basin, Mato Grosso, Brazil, in dorsal (top), lateral (middle), and ventral (below) views.

Diagnosis. *Hypostomus khimaera* is distinguished from its congeners, except for the species from the *H. cochliodon* group *sensu* Armbruster (2003), by of the following characteristics: (I) absence of a notch between the metapterygoid and the hyomandible (Fig. 2A) (*vs.* presence; see Armbruster, 2003:13, fig. 2A), (II) acutely angled dentaries, up to about 90° (*vs.* obtusely angled dentaries, generally forming a clearly angled greater than 90°), (III) teeth with medial cusp typically spatulate (*vs.* only villiform teeth); and (IV) exposed portion of opercle relatively small and completely bordered by a thick layer of skin (Fig. 3) (*vs.* exposed portion of opercle relatively large and not bordered by a thick layer of skin; see Armbruster, 2003:13, fig. 2A). *Hypostomus khimaera* is distinguished from species in the *H. cochliodon* group, except *H. basilisko* and *H. soniae* Hollanda Carvalho & Weber, 2005, by typically presenting a dark stripe along the median portion of the flank; diffuse in some specimens (*vs.* stripe absent); from *H. basilisko* and *H. soniae*, it differs by having dark spots on at least some region of the body (*vs.* body completely devoid of dark spots). Additionally, *H. khimaera* differs from *H. cochliodon*, *H. dardanelos* Zawadzki & Carvalho, 2014, *H. ericae* Hollanda Carvalho & Weber, 2005, *H. ericius* Armbruster, 2003, *H. labyrinthus* Oliveira, Ribeiro, Canto & Zawadzki, 2020, *H. oculus* (Fowler, 1943), *H. paucipunctatus* Hollanda Carvalho & Weber, 2005, *H. pyrinesei* (Miranda Ribeiro, 1920), *H. taphorni* (Lilyestrom, 1984) and *H. waiampi* Hollanda Carvalho & Weber, 2005 by having more externalized opercle, with exposed portion easily visible (*vs.* more internalized opercle, with exposed portion, when present, strongly reduced). It can be further distinguished from *H. pagei* Armbruster, 2003 by having fewer plates between the caudal and adipose fins (6–8 *vs.* 9–10); from *H. kopeyaka* Carvalho, Lima & Zawadzki, 2010 and *H. labyrinthus* by having only rounded dark spots on the body (*vs.* conspicuously horizontally elongated dark spots in addition to rounded dark spots in *H. kopeyaka*; dark vermiculated spots in addition to rounded dark spots in *H. labyrinthus*); from *H. oculus*, *H. plecostomoides* (Eigenmann, 1922) and *H. simios* Hollanda Carvalho & Weber, 2005 by having dark spots on the body in a clearly smaller number and more widely spaced even in the most spotted specimens (*vs.* body densely covered by closely spaced spots); from *H. levis* (Pearson, 1924) by having an adipose fin (*vs.* adipose fin absent); from *H. sculpodon* by having 26 to 28 plates in the median series of lateral plates (*vs.* 30).

Description. Morphometric data in Tab. 1. Head large, slightly compressed laterally. Snout and anterior profile generally subtriangular in dorsal view; slightly rounded in some specimens. Eye generally of moderate size, varying slightly in size in some individuals and positioned dorsolaterally. Dorsal margin of orbit elevated. Compound pterotic covered with well-developed odontodes in some individuals. Greater body width at cleithrum, gradually compressing towards base of caudal fin; in some specimens, compression more pronounced posteriorly to first four mid-ventral plates. Opercle partially exposed, completely bordered by thick layer of skin; covered by numerous odontodes; exposed portion small to moderate in size, typically irregular, with ellipsoid, rounded or teardrop shape (Figs. 2A, 3).

Dorsal profile of head almost straight from tip of snout to anterior margin of parieto-supraoccipital, forming angle of approximately 45° with ventral surface of head; convex from this point to origin of dorsal fin; sloping downwards from this point to first dorsal procurrent ray of caudal fin, rising again from this point to insertion of caudal fin.

TABLE 1 | Morphometric data of the holotype and 33 non-type specimens of *Hypostomus khimaera*. SD = Standard deviation.

	Holotype	Low–High	Mean±SD
Standard length	139.1	58.2–171.4	110.6±33.3
Percent of standard length			
Predorsal length	39.4	36.3–43.0	39.4±1.5
Head length	31.7	24.2–35.6	31.9±2.1
Interdorsal distance	20.5	18.7–22.4	20.4±1.0
Thoracic width	23.1	20.6–25.9	23.3±1.3
Abdominal width	22.5	19.9–23.9	21.7±0.9
Caudal peduncle length	33.8	31.0–36.6	33.3±1.3
Caudal peduncle depth	9.8	8.6–10.8	9.8±0.6
Dorsal-fin spine length	30.4	24.6–34.5	28.7±2.3
Dorsal-fin base length	25.3	22.7–28.3	25.9±1.4
Pectoral-fin spine length	30.6	26.4–31.4	28.6±1.4
Pelvic-fin spine length	25.5	21.7–27.8	24.6±1.3
Dorsal caudal-fin ray length	27.4	22.3–39.4	31.1±4.8
Ventral caudal-fin ray length	28.3	26.1–42.1	34.0±4.3
Adipose-fin spine length	6.4	4.3–10.8	6.5±1.2
Cleithral width	31.3	27.2–32.2	30.3±1.0
Percent of head length			
Head depth	70.5	55.1–87.2	64.2±6.0
Snout length	65.0	60.4–87.2	65.6±4.4
Interorbital width	45.6	41.4–61.3	46.4±3.6
Orbital diameter	16.6	14.2–23.8	16.8±1.8
Lower lip width	38.7	38.8–60.6	47.2±4.7
Lower lip length	7.6	9.8–18.2	13.4±2.1
Mandibular ramus length	15.0	11.7–20.2	14.9±2.4
Maxillary barbel length	7.6	5.0–12.8	8.7±1.7

Ventral profile varying from almost straight to slightly convex from tip of snout to insertion of unbranched ray of pelvic-fin; almost straight from this point to first ventral procurrent ray of caudal fin, descending to caudal-fin insertion. Caudal peduncle reduced and laterally compressed, wider in anterior region and very compressed posteriorly to insertion of adipose fin.

Oral disc rounded, sometimes ovoid, relatively small in size; lower lip not reaching transverse line through gill openings; ventral surface covered by numerous small papillae, decreasing in size posteriorly; odontodes generally present on almost entire surface of upper lip in adults; smaller specimens sometimes with wider naked region. Maxillary barbel equal to or slightly longer than eye pupil. Buccal papilla generally absent; papilla present and small in some specimens. Dentaries acutely angled, varying from about 70° to 90° between each ramus (average, 82°) (33); poorly preserved and/or stored specimens (especially those compressed into the jars) may variably appear to have an angle larger than 90° between dentary rami. Eight to 44 teeth (mode 32; 21*) in premaxillary, 9 to 39 teeth (mode 31; 22*) in dentary. Bicuspid teeth, with medial cusp generally shovel-shaped or spatulate (Figs. 2B–C); medial cusp varying from rounded to oblong in ventral view; conspicuously more developed than lateral cusp (Figs. 2B–C, 4); distinct and generally well-developed lateral cusp (Figs. 2B–C), sometimes fused with

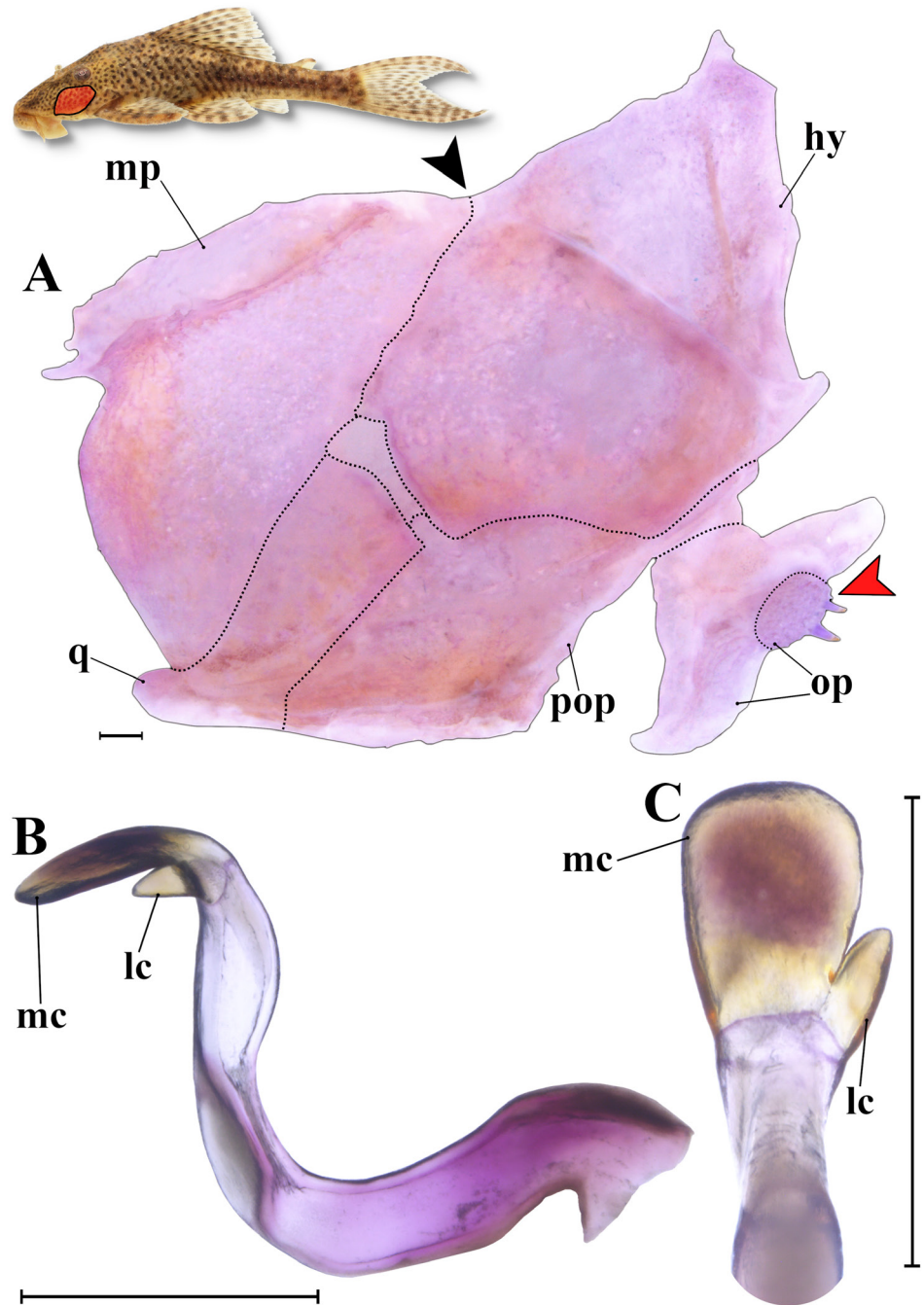


FIGURE 2 | Detail of suspensorium and most common morphological pattern of the teeth in *Hypostomus khimaera*. **A**. Black arrow showing absence of notch between hyomandibula and metapterygoid, red arrow indicating externalized portion of opercle; **B**. An entire premaxillary tooth in lateral view; and **C**. Detail of the inner surface of its distal portion, showing the typical shovel-shaped/spatulate medial cusp and a well-developed lateral cusp. Photo (**A**) from CITL 1152 (1 c&s, 117.9 mm SL), and (**B**) and (**C**) from CITL 1149 (1 c&s, 134.5 mm SL). Abbreviations: mp: metapterygoid, hy: hyomandibula, q: quadrate, pop: preopercle, op: opercle, lc: lateral cusp, mc: medial cusp. Scale bar = 1.0 mm.

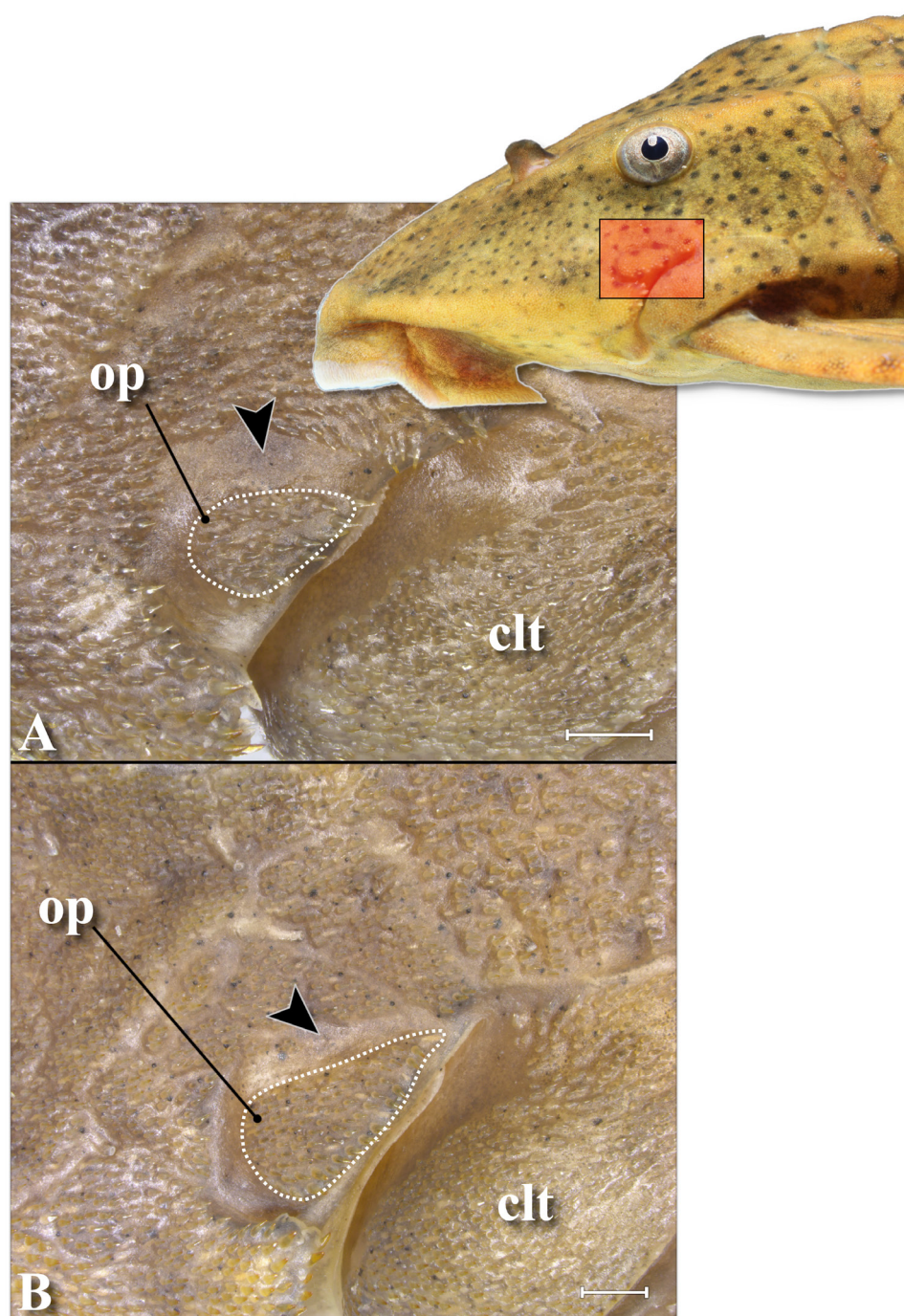


FIGURE 3 | External morphology of the operculum in *Hypostomus khimaera*, showing exposed portion of the smaller, roughly ellipsoid operculum in (A), CITL 1143, 90.5 mm SL, and exposed portion of the larger, teardrop-shaped operculum in (B), CITL 1143, 91.1 mm SL. Black arrows indicate the thick layer of skin that borders the externalized portion of the operculum (bordered by white dotted line). Areas shown in (A) and (B) highlighted in red in the miniature photo of the lateral portion of the head in a living specimen of *H. khimaera* (CITL 1156, 151.1 mm SL). Abbreviations: clt: cleithrum, op: operculum. Scale bar = 1.0 mm.

medial cusp (similar to condition found in *Hypostomus hemicochliodon*, see Armbruster (2003, 2004) and *H. soniae*, see Hollanda Carvalho, Weber (2004); rarely, some larger specimens (119.2 mm to 171.4 mm SL) with villiform medial cusp. Dentition of juvenile specimens (up to approximately 100.0 mm SL) with same morphological variations observed in adults (Fig. 4).

Body covered by dermal plates bearing odontodes, most concentrated on dorsal surface of head and in middle portion of dermal plates. Dorsal surface of snout covered by dermal plates, except for small naked area on snout tip. Mesethmoid region covered by more developed odontodes, forming median bulge from snout tip to nares. Conspicuous concentration of well-developed odontodes near nostril, passing through dorsal margin of orbit and extending through dorsal portion of compound pterotic, forming keels; less developed odontodes in some juvenile individuals. Predorsal region medially keeled; keels moderately developed, diverging slightly towards dorsal fin; less developed keels in some smaller individuals (up to about 100.0 mm SL). Dorsal surface of trunk covered by dermal plates except region around dorsal-fin. Lateral surface of trunk with five series of dermal plates on anterior portion of flanks and with four series

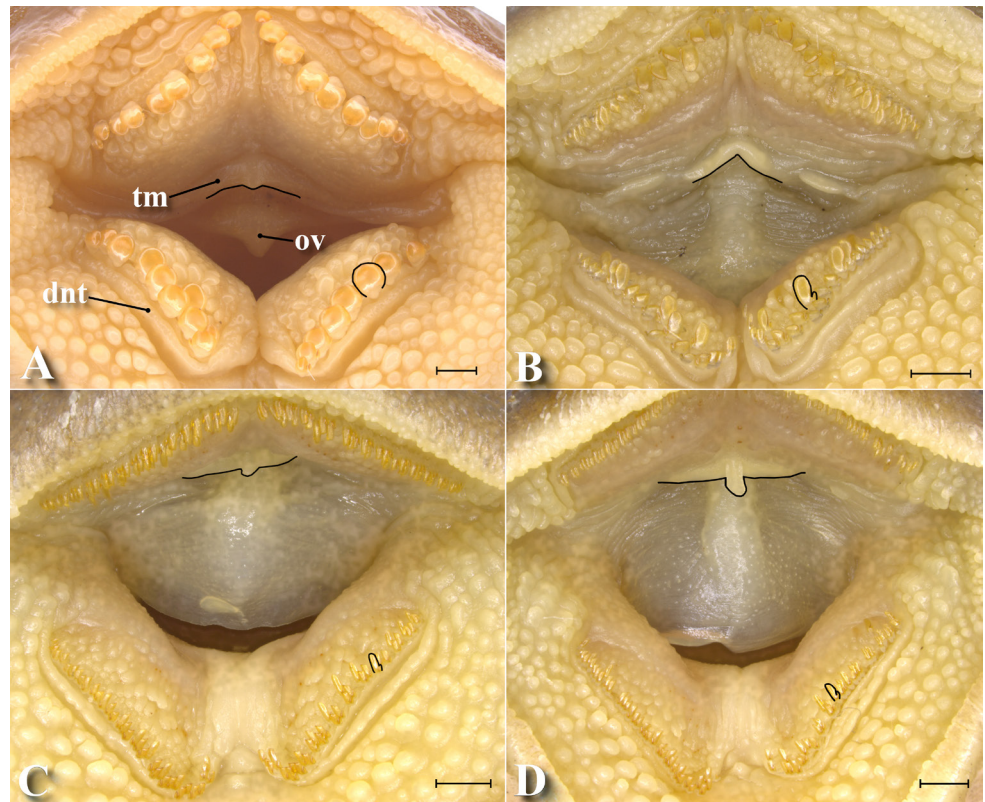


FIGURE 4 | Detail of the mouth of *Hypostomus khimaera* showing morphological variations in relation to the median buccal papilla and teeth. **A.** Specimen with poorly developed median buccal papilla and shovel-shaped teeth/spatulate teeth with wider medial cusp and nearly plain (CPUFMT 2561, 116.9 mm SL); **B.** Specimen devoid of median buccal papilla and with shovel-shaped/spatulate teeth (CITL 1148, 68.2 mm SL); **C.** Specimen with poorly developed median buccal papilla and villiform teeth (CITL 1143, 92.6 mm SL); and **D.** Specimen with developed buccal papilla and villiform teeth (CITL 1143 91.1 mm SL). Abbreviations: dnt: dentary, ov: oral veil, tm: transverse membrane. Scale bars = 1.0 mm.

of dermal plates on postdorsal portion. Dorsal and mid-dorsal series of plates generally with moderately developed keels, gradually becoming less developed posteriorly; some larger individuals (around 160.0 mm SL) with keels on dorsal and mid-dorsal series well developed (Fig. 5B). Median series with lateral line, generally lacking keels; keels, when present, poorly developed. Mid-ventral series with angled plates from first to fifth plate, with keels varying from little developed to moderately developed; keels absent posteriorly. Ventral surface of trunk covered by minute dermal plates in individuals greater than 80.0 mm SL, except on region around pectoral and pelvic fins. Ventral series smoothly angled ventrally towards posterior portion of caudal peduncle. Ventral surface of head covered by small bony plates, with exception of region around mouth.

Pre anal plate present and exposed. Median series with 26 to 28 (mode 27*) plates. Body covered dorsally by longitudinal series of two dermal plates in pre dorsal region, followed posteriorly by nuchal plate; plates between dorsal and adipose fins generally 6–8 (mode 7*); single specimen (CITL 1311, 118.7 mm SL) with 5; plates between adipose and caudal fins 6–8 (mode 7*), and plates at base of dorsal fin generally 6–8 (mode 7*).

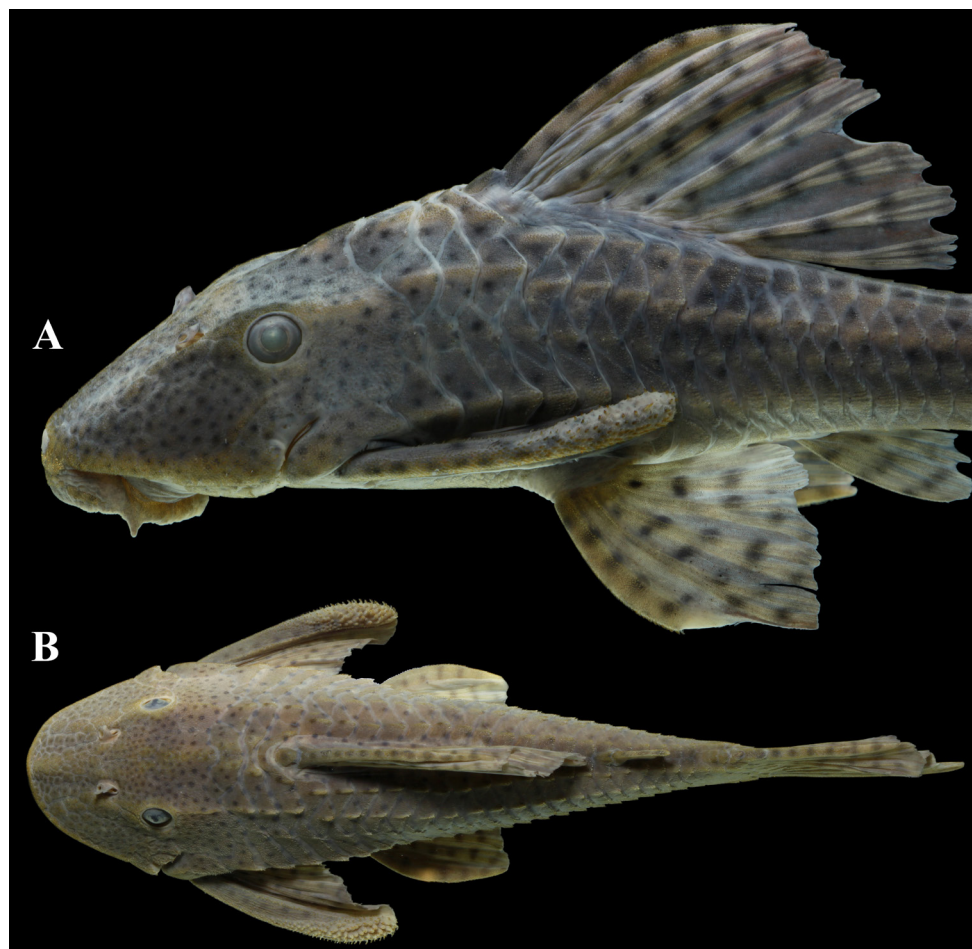


FIGURE 5 | Morphological variations in the keels of the dorsal and mid-dorsal series of bone plates in the anterior region of the trunk in *Hypostomus khimaera*, showing the most common pattern. **A.** With moderately developed keels (CITL 1161, 96.4 mm SL), and the infrequent pattern; **B.** With well-developed keels (ZUFMS-PIS 5277, 171.8 mm SL).

Dorsal fin II,7* (53), its origin at vertical through midpoint between pectoral and pelvic fins or slightly posterior to that point, usually passing halfway through second mid-ventral plate; region around dorsal-fin base naked; posterior margin straight or somewhat convex; posterior dorsal-fin rays not reaching adipose-fin spine when adpressed. Adipose-fin spine laterally compressed, ranging from almost straight to slightly curved inwards (Fig. 6). Pectoral fin I,6* (53), with almost straight posterior margin; pectoral-fin spine slightly curved inwards, covered by odontodes across its entire surface; anterior margin of spine with odontodes gradually becoming more developed towards tip of spine; dorsal surface of spine bearing poorly-developed odontodes with similar size, roughly aligned in longitudinal rows (relative to main axis of spine) on proximal two-thirds of spine, except for its posterior margin, which bears conspicuous line of odontodes gradually becoming more developed towards tip of spine; odontodes on distal portion of spine typically curved towards origin of spine in larger specimens (with more than 100.0 mm SL); ventral surface of spine mostly covered by poorly-developed odontodes with similar size, its distal portion with slightly more developed odontodes; tip of adpressed pectoral-fin spine reaching to anterior third of adpressed pelvic-fin spine. Pelvic fin i,5* (53), its posterior margin almost straight or slightly



FIGURE 6 | Specimens of *Hypostomus khimaera* in lateral view. **A.** Showing the adipose-fin spine almost straight (CITL 1153, 116.5 mm SL). **B.** Slightly curved inwards (CITL 1162, 151.1 mm SL). Part of the black dots on the caudal peduncle and pelvic and caudal fins in (A) are apparently related to an unidentified parasite.

convex; tip of adpressed spine extending beyond anal-fin origin. Anal fin $i,4^*$ (53), its distal margin reaching sixth bony plate posterior to its origin; unbranched rays and fifth branched ray smaller than second, third and fourth branched rays; third branched ray usually largest. Caudal fin $i,14,i^*$ (53); posterior margin furcated, with ventral lobe slightly larger than dorsal lobe; ventral lobe conspicuously larger than dorsal lobe in some individuals.

Coloration in alcohol. General color pattern in Figs. 1, 5–8, 11. Ground color of body generally ranging from light to dark yellowish brown; greyish brown in some specimens. Dark brown or black blotches on at least some region of body, typically with numerous closely spaced small rounded dark spots on head region (sometimes fused in some individuals), gradually becoming larger and more spaced posteriorly (Fig. 5B); in some individuals, dorsal surface of head may present sparse and diffuse black spots on snout, becoming more numerous and conspicuous in region posterior to eyes (compound pterotic and supraoccipital) (Figs. 1, 6A). Some specimens with darker background color, with few spots on body; dark blotches indistinct in intensely pigmented specimens, possibly due to melanism. Diffuse stripe between keels mid-dorsal and mid-ventral series of plates typically present, except for conspicuously dark specimens (possibly melanic) and specimens from córrego Boa Sentença, which apparently lack midline stripe. Ventral surface of trunk generally with small- to moderate-sized and roughly rounded dark brown or black blotches; some individuals devoid of or with sparse and diffuse blotches (Fig. 7). Ground color of fins similar to ground color of trunk, sometimes lighter; some specimens with ventral lobe of caudal fin slightly darker than dorsal lobe. Region around base of dorsal fin darker, extending medially along dorsal portion of caudal peduncle, generally forming diffuse dark band in dorsal region; color pattern of anal fin similar to that of dorsal fin, but dorsal fin generally darker. All fins generally covered with small, widely-spaced dark blotches; few, diffuse spots in some individuals; some specimens with conspicuous concentration of dark pigmentation on dorsal-fin membranes; some specimens with closely spaced dark blotches in pectoral and/or caudal fins, transversally aligned, forming dark bands. Color pattern of juvenile similar to that of adults and presenting same variations.

Coloration in life. Similar to color pattern of preserved specimens, with exception of dark stripe along midline of flank, which tends to be more evident. Background color of body yellowish brown in most all individuals; variably reddish brown, dark brown, greyish brown, or bright yellow (Fig. 8).

Sexual dimorphism. No sexual dimorphism was observed.

Geographical distribution. *Hypostomus khimaera* is widely distributed in the upper rio Paraguai basin within the Brazilian territory, occurring in the sub-basins of the rivers Aquidauana, Coxipó, Cuiabá, Manso, Jauru, Pari (LFCT, pers. obs.), Piquiri, Quilombo, Sepotuba, Taquari, Vermelho and Chacororé, in the states of Mato Grosso and Mato Grosso do Sul. Additionally, the species was recently recorded for the upper rio Paraná basin, in the córrego Mimoso, $21^{\circ}31'48''S$ $53^{\circ}26'47''W$, a tributary of the rio Anhanduí, southeastern Mato Grosso do Sul (Lopes *et al.*, 2024) (Fig. 9).



FIGURE 7 | Color pattern of ventral surface of the body in *Hypostomus khimaera*, showing some of the observed variations. **A.** CITL 1156, 151.1 mm SL, photographed alive; **B.** CITL 1140, 112.2 mm SL; **C.** CITL 1161, 85.1 mm SL; **D.** CITL 1160, 107.1 mm SL; **E.** CITL 1158, 123.4 mm SL; and **F.** CPUFMT 6040, 93.8 mm SL.

Ecological notes. *Hypostomus khimaera* is a species mainly found in streams and smaller rivers (Figs. 10A, B, D), but can be occasionally found in the main channel of larger rivers (Fig. 10C), commonly associated with marginal regions of lentic environments and sandy bottoms, especially with branches/trunks of submerged trees.

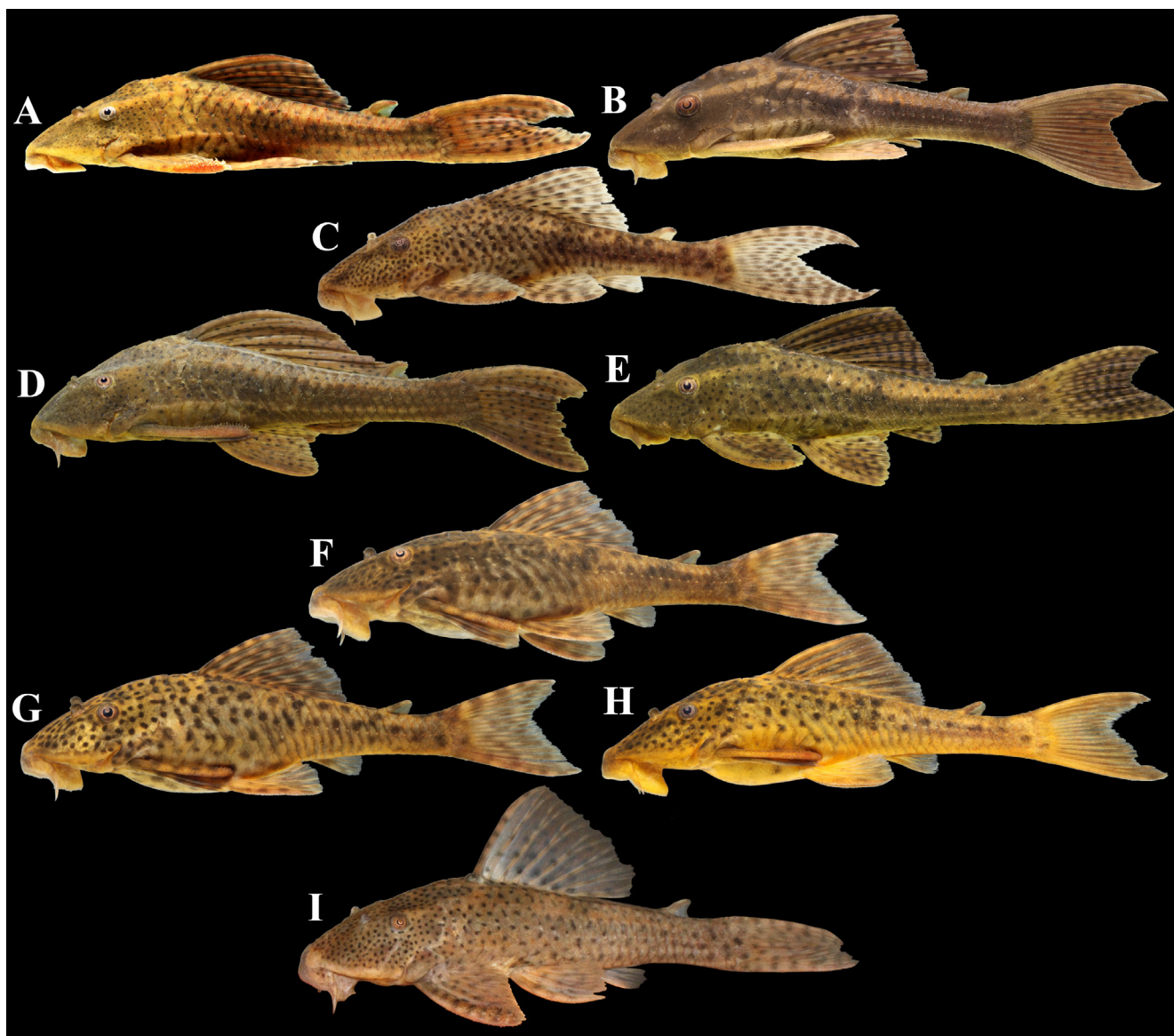


FIGURE 8 | General morphology and color pattern in life of *Hypostomus khimaera* in lateral view. **A.** CITL 1156, 151.1 mm SL, from the ribeirão Pedro Gomes, rio Piquiri basin; **B.** Uncatalogued, 100.0 mm SL, from the rio Curupira, a tributary of the rio Pari; **C.** Non-preserved specimen, 100.0 mm SL, from the córrego Criminoso, a tributary of the rio Taquari; **D.** 250.0 mm SL and **E.** 150.0 mm SL, both uncatalogued, from a tributary of the rio Juba, rio Sepotuba basin; **F, G** and **H.** uncatalogued specimens, all with approximately 100.0 mm SL, from the córrego Fortaleza, rio Taquari basin; **I.** CITL 1140, 130.0 mm SL, from the córrego Rio Verde, rio Taquari basin.

In headwater streams, small individuals of this species (up to approximately 100.0 mm SL) can also be found in lotic and shallow environments (up to around 20 cm depth), with a substrate composed by gravel, larger stones and sand. In the rio do Peixe, state of Mato Grosso do Sul, large specimens (about 250.0 mm SL) were found in lotic shallow environments (about 30 cm depth) and rocky substrate, with sections of slab, hiding under large boulders during the day, an atypical environment for a species from the *H. cochliodon* group (LFCT, 2024, pers. obs.). Like most loricariids, the species is more easily observed at night. Despite being part of the *H. cochliodon* group, the morphology

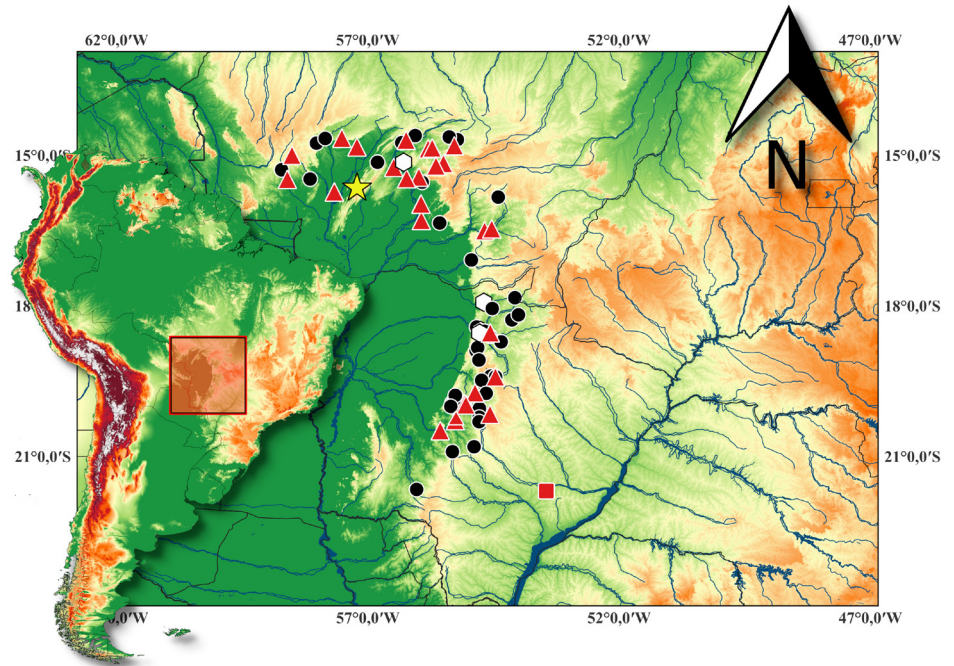


FIGURE 9 | Map showing the geographic distribution of *Hypostomus khimaera*: type-locality, the córrego Salobo (= Salobro), Mato Grosso (yellow star) and records from original description (red triangle). Additional records from this study (black circles) and records of specimens used for molecular analysis (white diamond). Record in the upper rio Paraná basin (red square). Each symbol can represent more than one location.

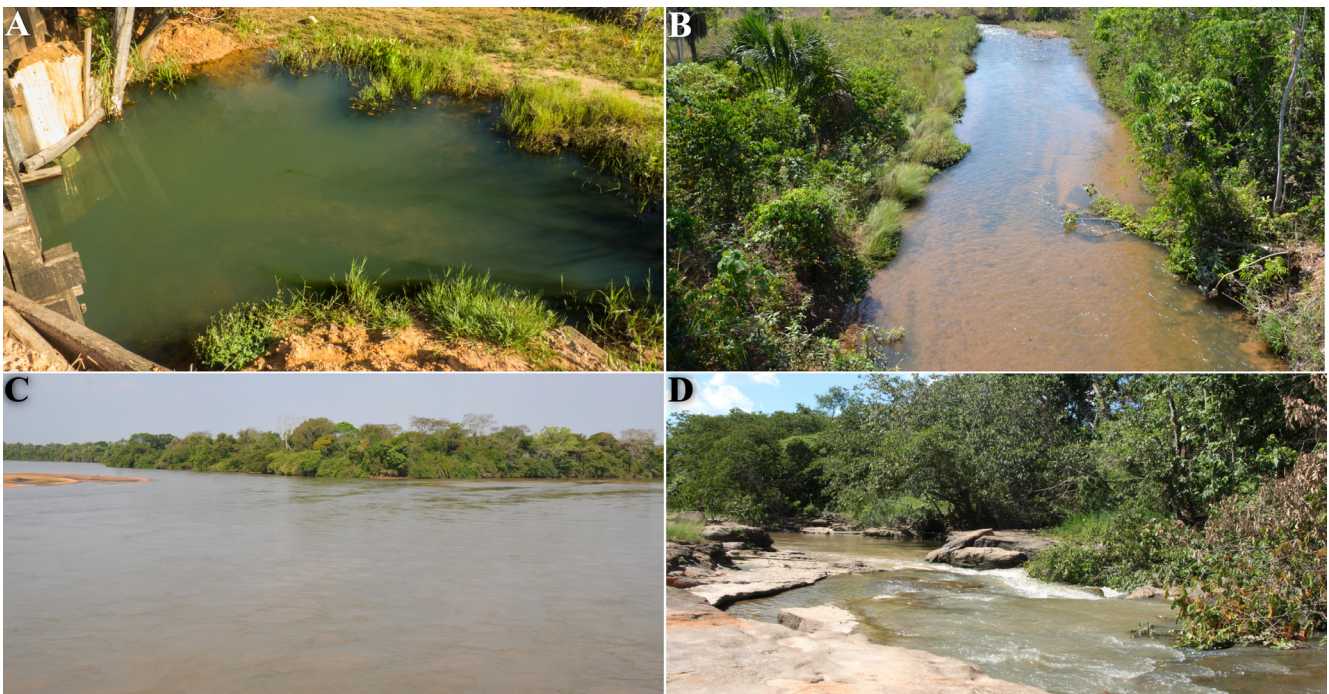


FIGURE 10 | Habitats of *Hypostomus khimaera*. **A.** Showing a small unnamed stream tributary of the rio Jatobá in Mato Grosso do Sul; **B.** Córrego Areia in Mato Grosso; **C.** Rio Taquari in Mato Grosso do Sul; and **D.** Córrego Onça, tributary of the rio Taquari. Photos by Otávio Froehlich (**A**), Hans Evers (**B** and **C**) and LFCT (**D**).

of its teeth is clearly different from the typical spoon-shaped pattern of xylophagous species (see Hollanda Carvalho, Weber, 2004: 960, fig. 4b, c), which combined with the common presence of specimens with strongly worn teeth suggests that the species may not be essentially xylophagous. The large morphological variations in body and dentition indicates that *H. khimaera* is possibly a species with presents high phenotypic plasticity, being opportunistic feeding habits, grazing both wood and periphytic matrix of rocky substrates.

Remarks. Despite being a considerably variable species in both morphology and color pattern, some populations are clearly more distinct from the expected range of variations in *Hypostomus khimaera*. Specimens from the córrego Fortaleza (Fig. 11A), a tributary of the rio Taquari in the region of Coxim, Mato Grosso do Sul, have a rounded snout in dorsal view (*vs.* roughly triangular, pointed), a reduced adipose fin (*vs.* well developed), and a comparatively shorter and more robust first rib (*vs.* longer and slender). Despite this, the fact that individuals with this peculiar morphological pattern occur only in this small tributary of the rio Taquari, and that specimens displaying similar morphology to the typical *H. khimaera* were also captured syntopically (see Fig. 8H), suggests that these individuals only represent another morphotype of *H. khimaera*. Other point that also raises doubts in this matter is the fact that the c&s individuals apparently have malformations in their ribs (from the second on), as well as other malformations in the cranium of some non c&s specimens. Furthermore, several collections in the rio Taquari main channel and smaller tributaries (see Material Examined section) revealed only individuals clearly compatible with the typical pattern of *H. khimaera*, which makes this issue even more complex. Despite the morphological differences raised herein, the number of individuals with this morphological pattern is relatively scarce, and broader integrative approaches are still necessary to better understand this population.

The population of the córrego Rio Verde (Fig. 11B), a tributary of the rio Verde in the municipality of Rio Verde de Mato Grosso, Mato Grosso do Sul, also presents morphological differences when compared to the typical *H. khimaera*, especially in larger individuals (larger than 120.0 mm SL): shorter and robust caudal peduncle, smoothly narrowing towards caudal-fin base in dorsal and lateral views (Fig. 8I) (*vs.* caudal peduncle typically longer, slender, clearly narrowing towards caudal-fin base (Figs. 8A–H)); rounded snout in dorsal view (*vs.* roughly triangular, pointed) and the cleithrum apparently wider than other individuals of the same size. Interestingly, smaller individuals (less than 120.0 mm SL) collected at this site have the typical morphology expected for juvenile *H. khimaera*. Additionally, even with the aforementioned morphological differences, larger specimens (with more than 120.0 mm SL) have the tooth pattern (*i.e.*, number and general morphology of medial cusp) compatible to the typical *H. khimaera*. In this sense, even though some morphological differences exist, important diagnostic features of *H. khimaera* are present in individuals from this population (*e.g.*, teeth morphology and number, opercle morphology, dark midline stripe, and dark blotches on body), which led us to consider it as one of the variable forms of *H. khimaera*.

A third distinct population was found in the córrego Boa Sentença (Fig. 11C), another tributary of the rio Verde, rio Taquari basin. Individuals from this population have comparatively larger dark blotches (*vs.* clearly smaller blotches), and apparently

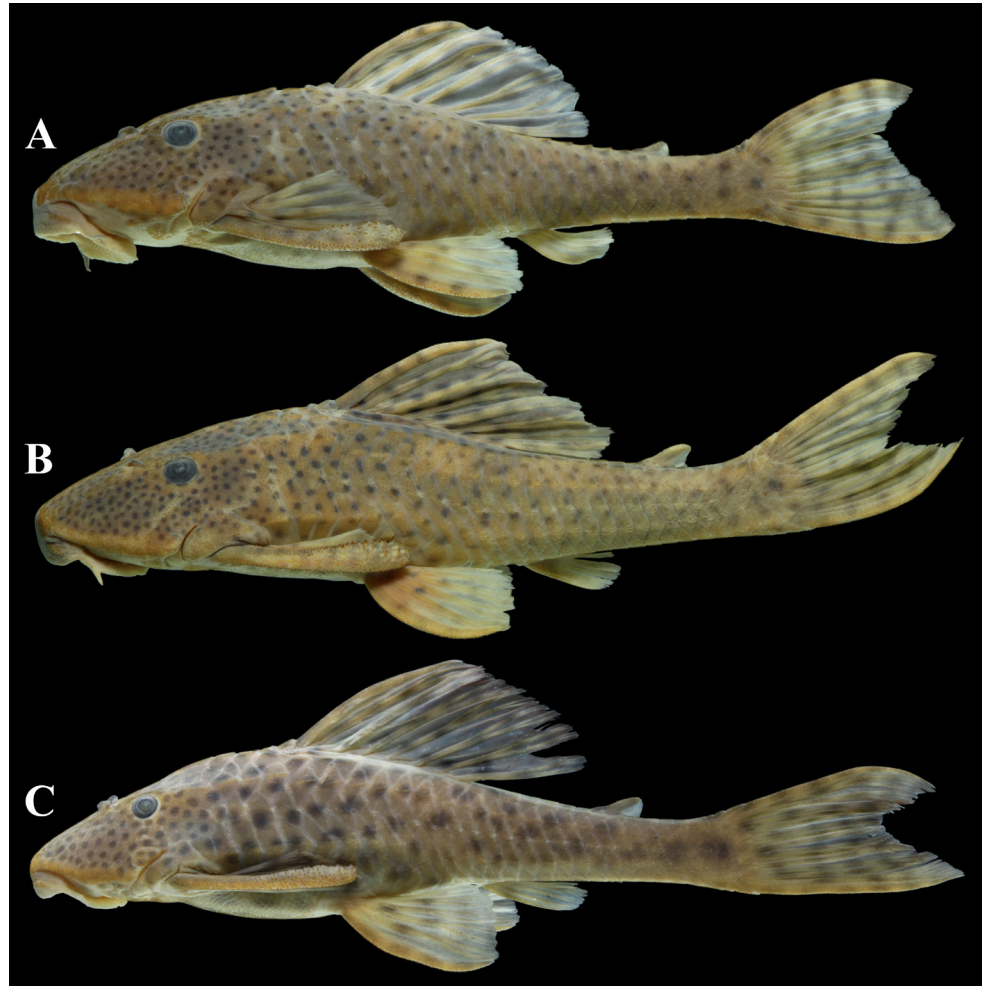


FIGURE 11 | Populations attributed to *Hypostomus khimaera* with conspicuous morphological differences. **A.** Specimen from the córrego Fortaleza (CITL 1160, 107.1 mm SL); **B.** Specimen from the córrego Rio Verde (CITL1140, 112.2 mm SL); and **C.** Specimen from the córrego Boa Sentença (CITL 1158, 123.4 mm SL), all from tributaries of the upper rio Paraguai basin in Mato Grosso do Sul.

lack the dark stripe along midline of flank (*vs.* midline stripe typically present and evident). Despite the apparent absence of the typical midline stripe in this population, it is important to mention that the available material is scarce, especially regarding adult specimens (largest specimen with about 120.0 mm SL). Therefore, new survey efforts in this drainage remain necessary to safely point the absence of the typical midlateral stripe as well as other putative diagnostic features, allowing us to undoubtedly confirm it as another variable form of *H. khimaera*. However, considering the overall similarity between the specimens from the córrego Boa Sentença and the typical *H. khimaera*, we opted to consider them conspecific herein. In any case, the dark longitudinal stripe along midline of flank is still extremely useful to distinguish *H. khimaera* from its congeners.

In the original description, the number of teeth (including both mandibular rami) was proposed as a diagnostic feature between *H. khimaera* (12 to 27 teeth) and *H. cochliodon* (7 to 9) (Tencatt *et al.*, 2014). However, our analysis demonstrates a wider

range for *H. khimaera* (8 to 44 teeth), overlapping with the known range of *H. cochliodon*. Notwithstanding, specimens of *H. khimaera* with eight or nine teeth variably presented unusually large gaps between teeth, suggesting tooth loss at these points. In any case, the absolute number of teeth was considered herein to standardize tooth count. The lower counts in tooth range falling within the range of *H. cochliodon* was found in specimens from different localities (e.g., CPUFMT 2561 and CPUFMT 8344), whereas the higher limit was found in specimens from the córrego Fortaleza (e.g., CITL 1159).

Even though it was possible to recognize some differences in color pattern and/or external morphology when comparing the populations from the córrego Fortaleza, córrego Rio Verde and córrego Boa Sentença (check previous paragraphs in this section), most of these putative diagnostic features are not exclusive, being variably present in individuals from other populations, although in lower frequency. In this sense, the most reasonable decision right now is to attribute these populations to *H. khimaera*, something that can eventually change as suitable diagnostic characters are discovered.

Molecular data. The analyses indicate that the sequences examined in this study form a cohesive molecular taxonomic unit (MOTU), identified morphologically as *Hypostomus khimaera* (Fig. 12). Furthermore, these analyses reveal that specimens from the córrego Fortaleza, the most morphologically distinct population when compared to typical *H. khimaera* (see Remarks), exhibit 0% of intraspecific genetic distance when compared to sequences of typical *H. khimaera* from other localities, such as the Cuiabá and Piquiri river basins (Tab. 2). *Hypostomus khimaera* exhibits a genetic distance exceeding 3% when compared to congeners previously deposited in the Genbank (Tab. 2).

Material examined. In addition to the material examined by Tencatt *et al.* (2014), a total of 636 specimens were examined, which are listed below. All from Brazil, upper rio Paraguai basin. **Mato Grosso.** CPUFMT 3028, 8, 101.7–146.6 mm SL; CPUFMT 3550, 5, 120.0–153.3 mm SL; CPUFMT 2729, 6, 118.4–135.3 mm SL; CPUFMT 2844, 3, 123.3–157.0 mm SL; CPUFMT 3417, 3, 103.7–132.7 mm SL; CPUFMT 2560, 2, 121.9–124.9 mm SL; CPUFMT 3016, 2, 90.4–90.9 mm SL; CPUFMT 3496, 1, 96.4 mm SL; CPUFMT 1454, 32, 59.0–125.3 mm SL; CPUFMT 4154, 1, 97.5 mm SL; CPUFMT 4171, 1, 80.6 mm SL; CPUFMT 183, 2, 46.4–47.3 mm SL; CPUFMT 160, 2, 78.5–85.2 mm SL; CPUFMT 3002, 2, 64.3–73.1 mm SL; CPUFMT 407, 1, 76.1 mm SL; CPUFMT 3164, 1, 111.6 mm SL; CPUFMT 1455, 3, 32.5–61.6 mm SL; CPUFMT 1503, 1, 124.1 mm SL; CPUFMT 2302, 1, 65.8 mm SL; CPUFMT 2367, 3, 109.2–132.9 mm SL; CPUFMT 4624, 1, 55.3 mm SL; CPUFMT 8344, 2, 65.6–81.1 mm SL; CPUFMT 8345, 1, 71.4 mm SL; CPUFMT 8346, 5, 47.8–57.2 mm SL; CPUFMT 8347, 5, 47.2–50.9 mm SL; CPUFMT 8348, 2, 72.23–77.1 mm SL. **Mato Grosso do Sul.** CITL 1137, 1, 58.2 mm SL; CITL1138, 1, 59.8 mm SL; CITL 1139, 66, 24.5–98.9 mm SL; CITL 1140, 33, 46.3–113.7 mm SL; CITL 1141, 5, 65.5–69.4 mm SL; CITL 1142, 9, 67.6–99.3 mm SL; CITL 1143, 3, 90.8–91.8 mm SL; CITL 1144, 5, 68.5–75.1 mm SL; CITL 1145, 2, 83.6–88.7 mm SL; CITL 1146, 4, 33.9–64.4 mm SL; CITL 1147, 17, 55.0–86.1 mm SL; CITL 1148, 2, 60.6–68.2 mm SL; CITL 1149, 1 c&s, 134.5 mm SL; CITL 1150, 7, 43.8–102.2 mm SL; CITL 1151, 2, 75.8–71.1 mm SL; CITL 1152, 1 c&s, 117.9 mm SL; CITL 1153, 3, 49.9–116.5 mm SL; CITL 1154, 1, 77.0 mm SL;

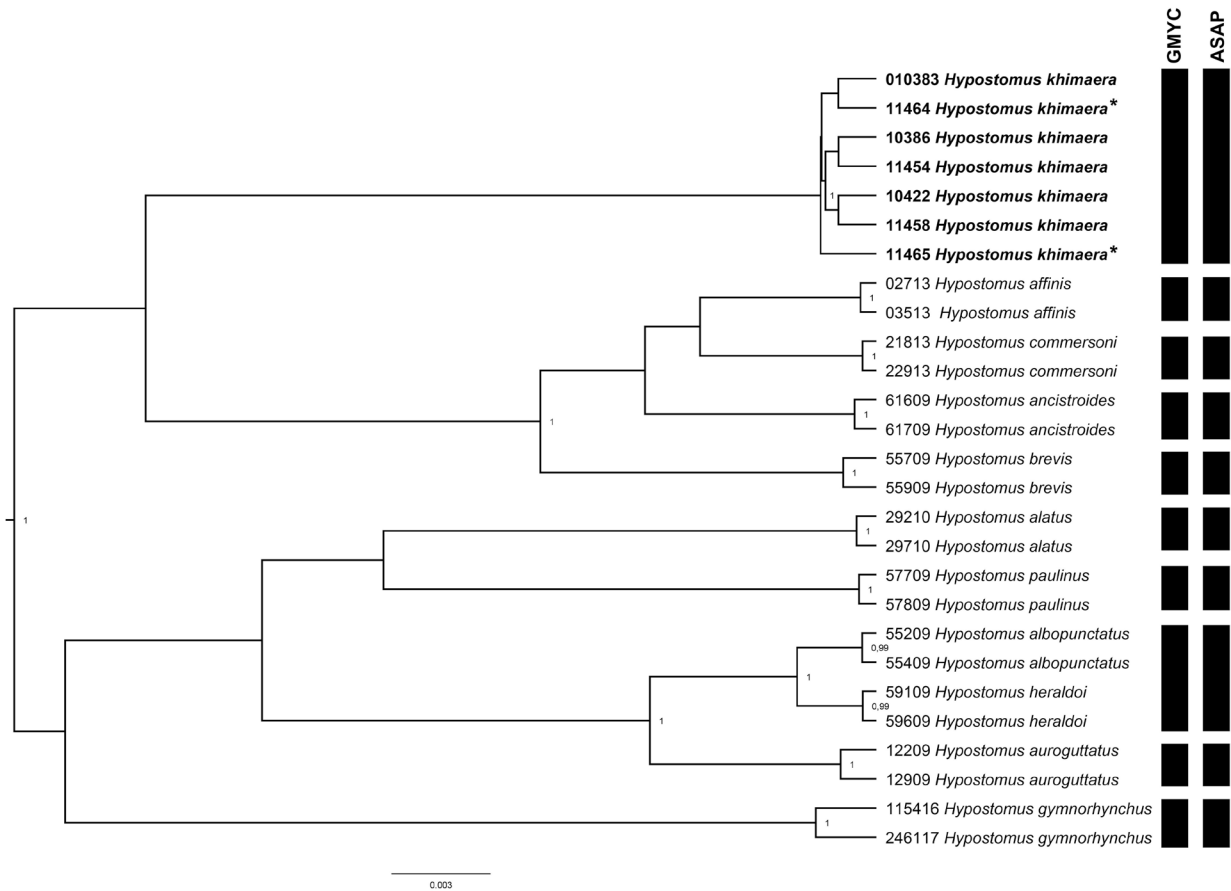


FIGURE 12 | Dendrogram including some populations of *Hypostomus khimaera*, constructed based on Bayesian Inference analysis of COI sequences. Sequences of *H. khimaera* were obtained in this study; sequences of the remaining congeners were obtained from BOLD. Specimens from the córrego Fortaleza, the most peculiar population attributed herein to *H. khimaera*, are indicated with asterisks. The black bars represent the Molecular Operational Taxonomic Units (MOTUs) formed by the species delimitation methods, Automatic Species Assembly Partitioning (ASAP), and the Generalized Mixed Yule Coalescent (GMYC).

TABLE 2 | Average genetic distances using the Cytochrome c Oxidase I gene based on the Kimura-2-Parameter model for analysis of intra (*) and interspecific distances of nominal species of *Hypostomus*.

<i>Hypostomus</i> species	1	2	3	4	5	6	7	8	9	10	11
1. <i>Hypostomus khimaera</i>	0*										
2. <i>Hypostomus paulinus</i>	4.56	0*									
3. <i>Hypostomus heraldoi</i>	5.14	4.32	0*								
4. <i>Hypostomus gymnorhynchus</i>	4.5	4.4	5.53	0*							
5. <i>Hypostomus commersoni</i>	3.84	4.51	5.64	4.58	0*						
6. <i>Hypostomus brevis</i>	4.72	4.96	5.83	5.13	2.23	0*					
7. <i>Hypostomus auroguttatus</i>	5.09	4.22	1.67	5.43	5.54	5.72	0*				
8. <i>Hypostomus ancistroides</i>	3.46	4.14	4.89	4.21	1.05	1.87	4.78	0*			
9. <i>Hypostomus albopunctatus</i>	5.4	4.51	0.52	5.72	5.84	6.02	1.49	5.08	0*		
10. <i>Hypostomus alatus</i>	4.42	2.48	3.2	3.84	4.13	4.67	3.11	3.77	3.39	0*	
11. <i>Hypostomus affinis</i>	4.22	4.5	5.25	4.58	1.4	2.23	5.15	1.04	5.44	4.13	0*

CITL 1155, 2, 65.4–91.2 mm SL; CITL 1156, 5, 125.5–151.1 mm SL; CITL 1157, 1, 93.4 mm SL; CITL 1158, 14, 55.5–123.8 mm SL; CITL 1159, 5 of 7, not measured; 2 c&s of 7, 96.0–112.2 mm SL; CITL 1160, 18, not measured; CITL 1161, 2, 85.12–96.4 mm SL; NUP 21369, 12, 28.0–95.0 mm SL; NUP 21426, 20, 28.0–63.0 mm SL; NUP 21459, 27, 22.0–62.0 mm SL; NUP 21628, 9, 40.0–122.0 mm SL; NUP 25433, 4, 68.2–77.7 mm SL. ZUFMS-PIS 1163, 9, 55.8–114.6 mm SL; ZUFMS-PIS 1566, 6, 29.8–63.7 mm SL; ZUFMS-PIS 1807, 4, 70.7–91.9 mm SL; ZUFMS-PIS 1881, 1, 82.5 mm SL; ZUFMS-PIS 1910, 1, 101.0 mm SL; ZUFMS-PIS 1965, 56, 26.1–69.2 mm SL; ZUFMS-PIS 1983, 12, 23.5–103.1 mm SL; ZUFMS-PIS 2034, 19, 27.4–69.1 mm SL; ZUFMS-PIS 3532, 1, 56.2 mm SL; ZUFMS-PIS 3550, 1, 60.1 mm SL; ZUFMS-PIS 3595, 2, 20.6–26.6 mm SL; ZUFMS-PIS 3833, 2, 88.0–101.4 mm SL; ZUFMS-PIS 3862, 1, 115.2 mm SL; ZUFMS-PIS 3874, 4, 42.7–89.0 mm SL; ZUFMS-PIS 3966, 7, 29.0–66.0 mm SL; ZUFMS-PIS 3967, 1, 38.8 mm SL; ZUFMS-PIS 3976, 2, 29.6–56.9 mm SL; ZUFMS-PIS 3982, 4, 32.7–42.4 mm SL; ZUFMS-PIS 4051, 3, 35.9–58.9 mm SL; ZUFMS-PIS 4219, 4, 31.1–44.1 mm SL; ZUFMS-PIS 4246, 7, 53.7–99.7 mm SL; ZUFMS-PIS 4255, 29, 40.4–89.0 mm SL; ZUFMS-PIS 4284, 1, 39.0 mm SL; ZUFMS-PIS 4319, 3, 64.4–142.2 mm SL; ZUFMS-PIS 4320, 2, 98.0–146.3 mm SL; ZUFMS-PIS 4324, 1, 91.6 mm SL; ZUFMS-PIS 4343, 2, 40.8–43.4 mm SL; ZUFMS-PIS 4357, 8, 42.6–78.3 mm SL; ZUFMS-PIS 4368, 49, 45.5–107.9 mm SL; ZUFMS-PIS 4465, 2, 48.2–53.3 mm SL; ZUFMS-PIS 4948, 1, 60.0 mm SL; ZUFMS-PIS 5037, 2, 53.3–71.7 mm SL; ZUFMS-PIS 5277, 6, 171.8 mm SL; ZUFMS-PIS 5949, 1, 33.3 mm SL; ZUFMS-PIS 5962, 11, 31.1–59.6 mm SL; ZUFMS-PIS 5976, 1, 46.9 mm SL.

Key to the species of *Hypostomus* from the Brazilian portion of the rio Paraguai basin (adapted from Tencatt, 2022)

- 1a. Exposed portion of opercle, when present, completely bordered by a thick layer of skin 2
- 1b. Exposed portion of opercle bordered by bony plates 4
- 2a. Dark spots absent on the body *H. basilisko*
- 2b. Dark spots present on the body 3
- 3a. Seven to nine teeth in each mandibular ramus; spoon-shaped medial cusp *H. cochliodon*
- 3b. 8 to 44 teeth on each mandibular ramus; medial cusp typically spatulate/shovel shaped; variably villiform *H. khimaera*
- 4a. Head and trunk with pale spots and/or transverse and/or diagonal pale bars 5
- 4b. Head and trunk with dark spots; spots variably diffuse or absent 6
- 5a. Posterior half of flanks with transverse pale bars *H. peckoltoides* (*and juveniles of *H. latifrons*)
- 5b. Posterior half of flanks lacking transversal pale bars *H. regani*
- 6a. Adipose fin absent *H. careopinnatus*
- 6b. Adipose fin present 7
- 7a. Unicuspid teeth *H. perdido*
- 7b. Bicuspid teeth 8
- 8a. Markedly wide body (dorsal view); unbranched caudal-fin rays conspicuously elongated, with size similar to predorsal length *H. ternetzi*

- 8b. Clearly narrower body (dorsal view); unbranched caudal-fin rays slightly to moderately elongated, with size similar to head length 9
- 9a. Three predorsal plates bordering the supraoccipital bone.....*H. latifrons*
- 9b. One predorsal plate bordering the supraoccipital bone..... 10
- 10a. Triangular snout in dorsal view; short dentaries; mid-dorsal series of bony plates with keels varying from moderately to well-developed *H. boulengeri*
- 10b. Rounded snout in dorsal view; dentaries varying from moderate to long in size; mid-dorsal series of bony plates with keels, when present, poorly developed..... 11
- 11a. Body densely covered with relatively small and closely spaced spots; dorsal and mid-dorsal series of lateral bony plates with moderately hypertrophied odontodes *H. renestoi*
- 11b. Body covered with relatively large and more spaced spots; dorsal and mid-dorsal series of lateral bony plates devoid of hypertrophied odontodes..... 12
- 12a. Mandibular ramus with 10 to 61 teeth 13
- 12b. Mandibular ramus with 68 to 111 teeth 14
- 13a. Blotches on head closely-spaced and relatively numerous; distance between adjacent blotches conspicuously smaller than diameter of blotches..... *H. froehlichii*
- 13b. Blotches on head more distant from each other and relatively fewer; distance between adjacent blotches similar to their diameter..... *H. fuscomaculatus*
- 14a. Head moderately compressed, with two parallel keels in the pre-dorsal region *H. latirostris*
- 14b. Head moderately depressed, lacking conspicuous keels in the pre-dorsal region *H. mutuae*

*Juvenile and adult individuals of *H. peckoltoides* Zawadzki, Weber & Pavanelli, 2010 can be distinguished from juveniles of *H. latifrons* Weber, 1986 by having only one predorsal plate bordering the supraoccipital bone (*vs.* three plates).

DISCUSSION

In the original description of *Hypostomus khimaera*, Tencatt *et al.* (2014:600) reported morphological variation among populations from different locations, especially regarding morphology of teeth and degree of development of odontodes and keels on trunk. To elucidate whether or not these different morphotypes represent a species complex, several populations within the rio Paraguai basin were analyzed for variations in color pattern, degree of odontode development, pattern of spots on the body and teeth traits.

The color pattern in the analyzed populations tends to be more conservative in individuals from the same location, however, as mentioned by Tencatt *et al.* (2014), it was possible to observe some degree of variation in specimens from the same location. According to Armbruster (2003), the color pattern is commonly variable in species of the *H. coeliodon* group, which limits its use in diagnoses. In *H. khimaera*, the intraspecific variation in the spot pattern is wide, including individuals with numerous and well-defined spots (Figs. 5B, 7) to individuals with scarce and diffuse spots (Fig. 6) (see Coloration in alcohol section).

Regarding the morphology of the teeth, Armbruster (2003, 2004) suggests that the most derived species of the *H. cochliodon* group evolved from an algivorous *Hypostomus*, reporting that the dentition of *H. hemicochliodon* presents an intermediate pattern between the species of the *H. cochliodon* group and other similar congeners. According to Tencatt *et al.* (2014), the teeth of *H. khimaera* tend towards a spoon-shaped pattern (except in juveniles, which have villiform teeth), with a shovel-shaped/spatulate medial cusp, which can vary from rounded to oblong. In fact, the spatulate pattern is the most common in larger individuals (over 100.0 mm SL) (Figs. 3, 4A). However, the analysis of new populations revealed that *H. khimaera* presents tooth pattern ranging from villiform to spatulate regardless of the size of the individual, although there is a clear tendency for small specimens (up to 100.0 mm CP) to have villiform teeth (Figs. 4B, C) and relatively large specimens (standard length over 150.0 mm) to have teeth with a spatulate medial cusp (Fig. 3). Even bearing villiform teeth in adult individuals, these specimens clearly belong to *H. khimaera*, and, as a consequence, to the *H. cochliodon* group by sharing the remaining diagnostic features of the group (see Diagnosis). When comparing the typical spoon/ladle-shaped teeth with the shovel-shaped/spatulate teeth, the most objective differences are that, in the first, the medial cusp is conspicuously concave with the lateral cusp tending to be reduced or even indistinct/absent, whereas medial cusp range from nearly plain, being short or wider to smoothly concave with a typically more pronounced lateral cusp in the later (Fig. 4).

Other morphological variations not mentioned by Tencatt *et al.* (2014) were observed herein, such as differences in the curvature of the adipose-fin spine, degree of exposure of the opercle, and presence/absence of buccal papilla. Hollanda Carvalho, Weber (2004) used the curvature of the adipose-fin spine to diagnose *H. ericae* from the other species of the group in their identification key, however, this characteristic proved to be variable in *H. khimaera*, with specimens having an adipose fin varying from almost straight to slightly curved inwards (Fig. 6). Regarding the exposed portion of the opercle, the most common pattern shows a relatively small and ellipsoid shape, although it is not uncommon to find individuals with a teardrop-shaped opercle (Fig. 2). Interestingly, a single analyzed specimen (CITL 1161, 96.4 mm SL) presents a thin layer of skin entirely covering the external portion of one of its opercles, making it not externally visible (Fig. 5A). The analysis of c&s individuals of *H. khimaera* make it clear that the size and shape of the external portion of the opercle is essentially related to the amount of skin that surrounds it, and not to the size and/or shape of the bone itself.

Armbruster (2003) had already used the presence of a small or absent buccal papilla *vs.* medium to large buccal papilla in his identification key to diagnose some species of the *H. cochliodon* group. The presence or absence of a buccal papilla was also used by Hollanda Carvalho, Weber (2004) to diagnose *H. waiampi* from *H. oculus* and *H. pyrineusi*. Regarding *H. khimaera*, the buccal papilla was considerably variable, with most specimens lacking it or, when having, varying from small- to moderate-sized (Fig. 4). During our study, it was possible to observe that this fragile, soft tissue structure, is easily damaged, generating doubts about whether it is really missing or was lost due to damage to the material. Therefore, we suggest that such characteristic should be used with caution in diagnoses of species from the *H. cochliodon* group.

The morphological variations observed in different populations of *H. khimaera* are probably associated with the wide distribution of this species, found in a diversity

of environments such as large river channels, streams and even headwater streams. Similarly, Tencatt *et al.* (2014) also suggested that there is a correlation with the sedentary characteristics of *Hypostomus* species, and that as a consequence, many populations that are geographically isolated in these different types of environments (especially in headwater streams) may present peculiar morphological variations. This type of interpopulational variation in widely distributed *Hypostomus* species has also been reported for relatively large species that mostly inhabit larger bodies of water, such as *H. albopunctatus* (Zawadzki *et al.*, 2019) and *H. hermanni* (Ihering, 1905) (Dias, Zawadzki, 2021). Even though there are conspicuous morphological differences between some individuals from different populations regarding a given character, the majority of specimens tend to present an intermediate pattern between the extremes observed and, even in more distinctive individuals, the existence of overlaps in most of the analyzed features is commonly observed. The presence of morphologically distinct conspecific specimens and/or populations with low genetical distance (see Remarks and Molecular data sections) highlights the importance of an integrative approach to better understand the limits of such highly variable and widespread species of *Hypostomus*.

Comparative material examined. In addition to the comparative material examined by Tencatt *et al.* (2014), the following specimens were examined. **Brazil.** *Hypostomus boulengeri* (Eigenmann & Kennedy, 1903), NUP 414, 3, 165.8–175.6 mm SL. *Hypostomus careopinatus* Martins, Marinho, Langeani & Serra, 2012, NUP 11257, 5, 30.2–53.8 mm SL. *Hypostomus fuscomaculatus* Zawadzki & Pains da Silva, 2022, NUP 22963, 223.5 mm SL, holotype. *Hypostomus froehlich* Zawadzki, Nardi & Tencatt, 2021, NUP 22689, 226.2 mm SL, holotype. *Hypostomus labyrinthus*, MNRJ 35631, 2 of 4, 70.7–72.7 mm SL, paratypes. *Hypostomus latifrons*, NUP 1039, 3, 240.0–260.0 mm SL. *Hypostomus latirostris* (Regan, 1904), BMNH 1892.4.20.26, 1, 159.3 mm SL, lectotype. *Hypostomus mutuae* Knaack, 1999, MCP 28669, 67.7 mm SL, holotype. *Hypostomus peckoltoides*, MZUSP 105226, 110.7 mm SL, holotype. *Hypostomus perdido* Zawadzki, Tencatt & Froehlich, 2014, MZUSP 111064, 159.1 mm SL. *Hypostomus regani* (Ihering, 1905), NUP 1032, 3, 260.0–270.0 mm SL. *Hypostomus renestoi* Zawadzki, Pains da Silva & Troy, 2018, NUP 12339, 1, 109.1 mm SL. *Hypostomus soniae*, MNRJ 35684, 2, 91.8–122.8 mm SL. *Hypostomus ternetzi* (Boulenger, 1895), BMNH 1895.5.17.64, 210.2 mm SL, holotype.

ACKNOWLEDGMENTS

The Universidade Estadual de Mato Grosso do Sul (UEMS) and the Universidade Federal de Mato Grosso do Sul provided logistical support. The authors are grateful to Fernando R. Carvalho (UFMS/ZUFMS), Francisco Severo-Neto and Thomaz Sinani (UFMS/ZUFMS) and Alexandre C. Ribeiro (UFMT/CPUFMT) for hosting museum visits and loaning of material and professor Marcelo Britto for their logistic support during the period of completion of this work in the Museu Nacional of the Universidade Federal do Rio de Janeiro. To Marcos Nunes for the unvaluable help on fieldwork. To Hans Evers and Markus Kaluza, for providing images of the *H. khimaera* in life. To Fernando Vaz-de-Mello, Jorge Arias and Andressa Bach from the Laboratório de Scarabaeoidologia (UFMT) for allowing the use and general support of the photomontage equipment Leica M205C (subproject EECBio UFMT/Finep #01.12.0359.00), respectively. CHZ received a grant from the Conselho Nacional de Desenvolvimento Científico

e Tecnológico (processes 313623/2018–0 and 434777/2018–8). To Tainá Barbosa de Souza, for the support in the molecular analyses. Authors were financially supported by the Coordenação de Aperfeiçoamento de Pessoal de Nível Superior (CAPES) (process 88887.902472/2023–00 to VCG), Conselho Nacional de Desenvolvimento Científico e Tecnológico (CNPq process 421733/2017–9 INAU II to DCF) and Fundação de Amparo à Pesquisa do Mato Grosso (process FAPEMAT–PRO.000339/2023 to DCF).

REFERENCES

- **Aljanabi SM, Martinez I.** Universal and rapid salt-extraction of high quality genomic DNA for PCR-based techniques. *Nucleic Acids Res.* 1997; 25(22):4692–93. <https://doi.org/10.1093/nar/25.22.4692>
- **Armbruster JW.** The species of the *Hypostomus cochliodon* group (Siluriformes: Loricariidae). *Zootaxa.* 2003; 249(1):1–60. <https://doi.org/10.11646/zootaxa.249.1.1>
- **Armbruster JW.** Phylogenetic relationships of the sucker mouth armored catfishes (Loricariidae) with emphasis on the Hypostominae and the Ancistrinae. *Zool J Linn Soc.* 2004; 141(1):1–80. <https://doi.org/10.1111/j.1096-3642.2004.00109.x>
- **Armbruster JW, Souza L.** *Hypostomus macushi*, a new species of the *Hypostomus cochliodon* group (Siluriformes: Loricariidae) from Guyana. *Zootaxa.* 2005; 920(1):1–12. <https://doi.org/10.11646/zootaxa.920.1.1>
- **Arruda PSS, Ferreira DC, Oliveira C, Venere PC.** DNA barcoding reveals high levels of divergence among mitochondrial lineages of *Brycon* (Characiformes, Bryconidae). *Genes.* 2019; 10(9):639. <https://doi.org/10.3390/genes10090639>
- **Boeseman M.** The genus *Hypostomus* Lacépède, 1803, and its Surinam representatives (Siluriformes: Loricariidae). *Zool Verh.* 1968; 99:1–89.
- **Brown SDJ, Collins RA, Boyer S, Lefort M-C, Malumbres-Olarte J, Vink CJ, Cruickshank RH.** Spider: an R package for the analysis of species identity and evolution, with particular reference to DNA barcoding. *Mol Ecol Resour.* 2012; 12(3):562–65. <https://doi.org/10.1111/j.1755-0998.2011.03108.x>
- **Carvalho GV, Santos M, Tencatt LFC.** Peixe da vez, *Hypostomus khimaera* Tencatt, Zawadzki & Froehlich, 2014. *Bol Soc Bras Ictiol.* 2019; 130:50–52.
- **Dias AC, Zawadzki CH.** *Hypostomus hermanni* redescription and a new species of *Hypostomus* (Siluriformes: Loricariidae) from Upper Paraná River basin, Brazil. *Neotrop Ichthyol.* 2021; 19(2):e200093. <https://doi.org/10.1590/1982-0224-2020-0093>
- **Fricke R, Eschmeyer WN, Fong JD.** Eschmeyer’s catalog of fishes: species by family/subfamily [Internet]. San Francisco: California Academy of Science; 2024. Available from: <https://researcharchive.calacademy.org/research/ichthyology/catalog/SpeciesByFamily.asp>
- **Hebert PDN, Stoeckle MY, Zemlak TS, Francis CM.** Identification of birds through DNA barcodes. *PLoS Biol.* 2004; 2(10):e312. <https://doi.org/10.1371/journal.pbio.0020312>
- **Hollanda Carvalho P, Weber C.** Five new species of the *Hypostomus cochliodon* group (Siluriformes: Loricariidae) from middle and lower Amazon System. *Rev suisse Zool.* 2004; 111(4):953–78.
- **Hollanda Carvalho P, Lima FCT, Zawadzki CH.** Two new species of the *Hypostomus cochliodon* group (Siluriformes: Loricariidae) from the rio Negro basin in Brazil. *Neotrop Ichthyol.* 2010; 8(1):39–48. <https://doi.org/10.1590/S1679-62252010000100006>
- **Jones M, Ghoorah A, Blaxter M.** jMOTU and taxonator: turning DNA barcode sequences into annotated operational taxonomic units. *PLoS ONE.* 2011; 6(4):e19259. <https://doi.org/10.1371/journal.pone.0019259>

- **Kearse M, Moir R, Wilson A, Stones-Havas S, Cheung M, Sturrock S, Buxton S, Cooper A, Markowitz S, Duran C, Thierer T, Ashton B, Meintjes P, Drummond A.** Geneious Basic: an integrated and extendable desktop software platform for the organization and analysis of sequence data. *Bioinformatics*. 2012; 28(12):1647–49. <https://doi.org/10.1093/bioinformatics/bts199>
- **Kimura M.** A simple method for estimating evolutionary rates of base substitutions through comparative studies of nucleotide sequences. *J Mol Evol*. 1980; 16:111–20.
- **Lopes DA, Souza RN, Gomes VC, Carvalho FR, Zawadzki CH, Tencatt LFC.** *Hypostomus khimaera* Tencatt, Zawadzki & Fröhlich, 2014 (Siluriformes, Loricariidae) in upper rio Paraná basin, Brazil: first record and comments about its occurrence. *Check List*. 2024; 20(3):594–600. <https://doi.org/10.15560/20.3.594>
- **McDonald R, Zhang F, Watts JEM, Schreier HJ.** Nitrogenase diversity and activity in the gastrointestinal tract of the wood-eating catfish *Panaque nigrolineatus*. *ISME*. 2015; 9(12):2712–24. <https://doi.org/10.1038/ismej.2015.65>
- **Monaghan MT, Wild R, Elliot M, Fujisawa T, Balke M, Inward DJG, Lees DC, Ranaivosolo R, Eggleton P, Barraclough TG, Vogler AP.** Accelerated species inventory on Madagascar using coalescent-based models of species delineation. *Syst Biol*. 2009; 58(3):298–311. <https://doi.org/10.1093/sysbio/syp027>
- **Oliveira RR, Ribeiro FRV, Canto ALC, Zawadzki CH.** A new species of the Neotropical loricariid of *Hypostomus cochliodon* group (Hypostominae) from the lower Rio Tapajós basin, Brazilian Amazon. *J Fish Biol*. 2020; 97(2):490–98. <https://doi.org/10.1111/jfb.14399>
- **Oyakawa OT, Akama A, Zanata AM.** Review of the genus *Hypostomus* Lacépède, 1803 from rio Ribeira de Iguape basin, with description of a new species (Pisces, Siluriformes, Loricariidae). *Zootaxa*. 2005; 921(1):1–27. <https://doi.org/10.11646/zootaxa.921.1.1>
- **Penido IS, Pessali TC, Zawadzki CH.** A new tiny-spotted species of *Hypostomus* (Siluriformes: Loricariidae) from the upper Rio Tocantins basin, Gois State, Brazil. *Zootaxa*. 2023; 5361(1):103–13. <https://doi.org/10.11646/zootaxa.5361.1.5>
- **Puillandre N, Brouillet S, Achaz G.** ASAP: Assemble species by automatic partitioning. *Mol Ecol Resour*. 2021; 21(2):609–20. <https://doi.org/10.1111/1755-0998.13281>
- **R Development Core Team.** R: A language and environment for statistical computing [Internet]. Vienna: R Foundation for Statistical Computing; 2016. Available from: <http://www.R-project.org/>
- **Reis RE, Kullander SO, Ferraris CJ Jr., editors.** Check list of the freshwater fishes of South and Central America. Porto Alegre: Edipucrs; 2003.
- **Sabaj MH.** Codes for natural history collections in ichthyology and herpetology. *Copeia*. 2020; 108(3):593–669. <https://doi.org/10.1643/ASIHCONDONS2020>
- **Schaefer SA.** Osteology of *Hypostomus plecostomus* (Linnaeus) with a phylogenetic analysis of the loricariid subfamilies (Pisces: Siluroidei). *Los Angeles County Mus Contrib Sci*. 1987; 394:1–31.
- **Schaefer SA.** The Neotropical cascudinhos: systematics and biogeography of the *Otocinclus* catfishes (Siluriformes: Loricariidae). *Proc Acad Nat Sci Philadelphia*. 1997; 148:1–120.
- **Schaefer SA, Stewart DJ.** Systematics of the *Panaque dentex* species group (Siluriformes: Loricariidae), wood-eating armored catfishes from tropical South America. *Ichthyol Explor Freshw*. 1993; 4(4):309–42.
- **Tamura K, Stecher G, Kumar S.** MEGA11: Molecular Evolutionary Genetics Analysis Version 11. *Mol Biol Evol*. 2021; 38(7):3022–27. <https://doi.org/10.1093/molbev/msab120>
- **Taylor WR, Van Dike GC.** Revised procedures for staining and clearing small fishes and other vertebrates for bone and cartilage study. *Cybio*. 1985; 9(2):107–19.

- **Tencatt LFC, Zawadzki CH, Froehlich O.** Two new species of the *Hypostomus cochliodon* group (Siluriformes: Loricariidae) from the rio Paraguay basin, with a redescription of *Hypostomus cochliodon* Kner, 1854. *Neotrop Ichthyol.* 2014; 12(3):585–602. <https://doi.org/10.1590/1982-0224-20130162>
- **Tencatt LFC.** Chaves: Siluriformes, Loricariidae, Chave para as espécies de *Hypostomus*. In: Gimênes Jr. H, Rech R, organizers. *Guia ilustrado dos peixes do Pantanal e entorno*. Campo Grande: Julien Design, 2022. p.614–15.
- **Thompson JD, Gibson TJ, Higgins DG.** Multiple sequence alignment using ClustalW and ClustalX. *Curr Protoc Bioinf.* 2003; 00:1–22. <https://doi.org/10.1002/0471250953.bi0203s00>
- **Ward RD.** DNA barcode divergence among species and genera of birds and fishes. *Mol Ecol Resour.* 2009; 9(4):1077–85. <https://doi.org/10.1111/j.1755-0998.2009.02541.x>
- **Weber C.** *Hypostomus dlouhyi*, nouvelle espèce de poisson-chat cuirassé du Paraguay (Pisces, Siluriformes, Loricariidae). *Rev suisse Zool.* 1985; 92(4):955–68.
- **Zawadzki CH, Birindelli JLO, Lima FCT.** A new pale-spotted species of *Hypostomus Lacépède* (Siluriformes: Loricariidae) from the rio Tocantins and rio Xingu basins in central Brazil. *Neotrop Ichthyol.* 2008; 6(3):395–402. <https://doi.org/10.1590/S1679-62252008000300012>
- **Zawadzki CH, Hollanda Carvalho P.** A new species of the *Hypostomus cochliodon* group (Siluriformes: Loricariidae) from the rio Aripuanã basin in Brazil. *Neotrop Ichthyol.* 2014; 12(1):43–51. <https://doi.org/10.1590/S1679-62252014000100004>
- **Zawadzki CH, Hollanda Carvalho P, Birindelli JL, Azevedo FM.** *Hypostomus nigrolineatus*, a new dark-striped species from the rio Jequitinhonha and rio Pardo basins, Brazil (Siluriformes, Loricariidae). *Ichthyol Explor Freshw.* 2016; 27(3):263–74.
- **Zawadzki CH, Silva HP, Troy WP.** Redescription of *Hypostomus latirostris* (Regan, 1904) with the recognition of a new species of *Hypostomus* (Siluriformes: Loricariidae) from the upper rio Paraguay basin, Brazil. *Ichthyol Explor Freshw.* 2018; 1079:1–18. <http://doi.org/10.23788/IEF-1079>
- **Zawadzki CH, Tencatt LFC, Britski HA.** Taxonomic revision of *Hypostomus albopunctatus* (Siluriformes: Loricariidae) reveals a new piece of the *Hypostomus jigsaw* in the upper Rio Paraná basin. *J Fish Biol.* 2020a; 6(1):230–42. <https://doi.org/10.1111/jfb.14209>
- **Zawadzki CH, Oliveira RR, Oliveira AS, Rapp Py-Daniel L.** Redescription of *Hypostomus carinatus* (Steindachner 1881) (Siluriformes: Loricariidae) from the rio Amazonas basin in Brazil. *Zootaxa.* 2020b; 4750(2):191–203. <https://doi.org/10.11646/zootaxa.4750.2.3>

AUTHORS' CONTRIBUTION

Vandergleison de Carvalho: Conceptualization, Data curation, Formal analysis, Investigation, Methodology, Project administration, Supervision, Validation, Visualization, Writing-original draft, Writing-review and editing.

Victória Joana da Silva Müller: Formal analysis, Investigation, Methodology, Validation, Writing-review and editing.

Daniela Cristina Ferreira: Formal analysis, Investigation, Methodology, Validation, Visualization, Writing-review and editing.

Cláudio Henrique Zawadzki: Data curation, Formal analysis, Investigation, Methodology, Supervision, Validation, Visualization, Writing-review and editing.

Luiz Fernando Caserta Tencatt: Conceptualization, Data curation, Formal analysis, Funding acquisition, Investigation, Methodology, Project administration, Resources, Supervision, Validation, Visualization, Writing-review and editing.

Neotropical Ichthyology



This is an open access article under the terms of the Creative Commons Attribution License, which permits use, distribution and reproduction in any medium, provided the original work is properly cited.

Distributed under
Creative Commons **CC-BY 4.0**

© 2024 The Authors.
Diversity and Distributions Published by SBI



Official Journal of the
Sociedade Brasileira de Ictiologia

ETHICAL STATEMENT

Part of the examined material was collected under the licences: #73139-3, #73139-2, #45578-7 and #85671-2, sent by Sistema de Autorização e Informação em Biodiversidade (SISBio) to LFCT.

COMPETING INTERESTS

The author declares no competing interests.

HOW TO CITE THIS ARTICLE

- **Carvalho V, Müller VJS, Ferreira DC, Zawadzki CH, Tencatt LFC.** Revisiting *Hypostomus khimaera* (Siluriformes: Loricariidae): the identity of a morphologically variable species. *Neotrop Ichthyol.* 2024; 22(3):e240057. <https://doi.org/10.1590/1982-0224-2024-0057>